LAWRENCE
LIVERMORE
NATIONAL
LABORATORY

LLNL-JRNL-643805

Boron-loaded Plastic Scintillator with Neutron-Gamma Pulse Shape Capability

I. A. Pawelczak, A. M. Glenn, H. P. Martinez, M. L. Carman, N. P. Zaitseva, S. A. Payne

September 17, 2013

Nuclear Instruments and Methods A

Disclaimer

Boron-loaded Plastic Scintillator with Neutron-γ Pulse Shape Discrimination Capability

I.A. Pawełczak, A.M. Glenn, H.P. Martinez, M.L. Carman, N.P. Zaitseva, S.A. Payne

Lawrence Livermore National Laboratory, Livermore, CA 94550

Abstract

Development of plastic scintillator with neutron sensitivity from thermal to multi-MeV and pulse shape discrimination (PSD) has been demonstrated. Incorporation of ^{10}B-containing compounds into plastic scintillator with PSD capability leads to detector improvement in regards to neutron detection efficiency while preserving the discrimination between neutrons and γ-rays. Effects of boron loading on scintillation and pulse shape discrimination properties are discussed. PSD figure-of-merit value of 1.4±0.03 has been achieved for events in thermal neutron energy domain, 50-100keV$_{ee}$, for PSD plastic loaded with 5wt.% of m-carborane.

Keywords: ^{10}Boron-loaded PSD plastic scintillator, Pulse shape discrimination, Thermal-neutron detection, Fast-neutron detection

1. Introduction

Neutron count rates, multiplicity and energy distributions serve as an indicator for the presence of Special Nuclear Material (SNM). Therefore, efficient solid-state neutron detectors with fast response and large active volume are in high demand for neutron detection in nuclear security and safeguards applications. Conventional technologies for neutron detection are based on ^{3}He for thermal-neutron detection, and liquid scintillators for fast-neutron detection. However, due to the shortage of ^{3}He supplies and the difficulty of handling and safety issues associated with liquid scintillators, new alternatives are under consideration. In addition, field deployment imposes a

☆LLNL-JRNL-643805

stringent requirement on detector operation in a self-triggering mode, and therefore detector internal ability to identify and distinguish neutrons from a γ-rays.

Studies of pulse shape discrimination phenomena in organic crystals and liquids led to the development of plastic scintillators with pulse shape discrimination (PSD) [1]. Incorporation of efficient thermal neutron converters such as ^{10}B or ^{6}Li into plastic scintillators with PSD capability increases neutron detection efficiency while discriminating neutrons from γ-rays on an event-by-event basis. Recent research has shown that ^{6}Li-loaded PSD plastics provide discrimination among thermal neutrons, fast neutrons and γ-rays [2], however the larger ^{10}B thermal neutron cross-section and ease of loading allow for significantly higher thermal neutron capture efficiency than for ^{6}Li-loaded plastic of the same size. Nonetheless, boron loaded PSD plastics are best suited to smaller size detectors due to the lower reaction Q-value, so ^{6}Li and ^{10}B loaded PSD plastics represent complementary technologies. In this manuscript, the sensitivity of PSD plastic scintillator to thermal neutrons is achieved by using the capture reaction on a nucleus of ^{10}B, according to [3]:

$$^{10}B + n = \begin{cases} ^{7}Li +^{4} He, & \text{Q=2.792MeV, 6\%,} \\ ^{7}Li +^{4} He + \gamma(480keV), & \text{Q=2.310MeV, 94\%.} \end{cases} \quad (1)$$

^{10}B loading was selected due to the high cross-sections for thermal neutron capture (72% of ^{3}He), high natural abundance (19.8%), emission of light charged particles in thermal neutron capture reaction, and chemical compatibility with plastic formulation. It is known that charged reaction products, (^{7}Li and ^{4}He), require only several tens of μm to be stopped in the scintillator. Their short range is desired for achieving good efficiency in a reasonable size detector. The ^{7}Li and ^{4}He products also have significantly different stopping power, dE/dx, from minimum ionizing particles such as recoiled electrons (γ-rays) which enhances PSD.

A boron-containing PSD plastic detects fast neutrons by recoiled protons and thermal neutrons by capture reaction products while discriminating against background γ-rays. The scintillator serves dual purposes as a detector and neutron moderator due to its high hydrogen content. This allows for accounting of neutrons which are below the detection threshold by recoiled protons and above the effective capture by thermal neutron converters. Neutrons thermalized within the detector volume diffuse until captured by ^{10}B or escape from the detector. This approach may allow for efficient detection

of fission neutrons with a compact detector design where external moderator is not required.

Moreover, detection of a multi-MeV neutron by a recoiled proton followed by detection of the capture reaction products within the scintillator provides additional information. Time correlated signals, fast generated due to recoiled proton, and diffusion delayed due to neutron capture, ensure neutron full energy deposition to the scintillator and provide improved neutron spectroscopy [4, 5, 6, 7]. Such a detector may be also considered to provide multiplicity information for neutron bursts [8] in a cost-effective way.

Organic liquid scintillators containing ^{10}B compounds have been used in the past for thermal neutron detection [9, 10]. High flash point liquid scintillators with PSD [11, 12, 13, 14, 15] were investigated for border monitoring applications and reported efficiency comparable to ^{3}He counters, although with significantly lower γ-ray rejection levels. On the other hand, solid state scintillators containing natural boron (glass, plastic and silicon rubber based) have been considered mainly as materials without PSD capability [16, 17, 18]. Existing boron-containing plastic scintillators without PSD use energy deposition, pulse height (PH), specific to charged reaction products, to identify neutrons. Such scintillators would benefit from the addition of PSD to provide additional rejection of omnipresent γ-rays events underneath the thermal neutron PH distribution.

The work presented in this paper is focused on the development of PSD plastic scintillator loaded with ^{10}B. Such a detector provides sensitivity to neutrons in a wide dynamic range and pulse shape discrimination capability. Furthermore, influences of m-carborane concentration, a compound used to introduce boron into plastic, on scintillator light emission properties and pulse shape discrimination are reported.

2. Experimental Methods and Simulation Calculations

Samples of PSD plastic containing varied concentrations of boron were made as colorless, optically transparent scintillators by dissolution of m-carborane, 28% of PPO (2,5-diphenyloxazole) and 0.2% of DPA (9,10-diphenylanthracene) into vinyltoluene or styrene. Carborane was used as a boron-containing compound because of its highest concentration of boron atoms per molecule among all known compounds compatible with organic scintillators. Natural abundance of boron in m-carborane was used due to significantly lower cost than

its enriched form. Performance tests of synthesized plastic scintillator samples with respect to neutrons were carried out in the presence of γ-rays using a ^{252}Cf source. In order to attenuate the flux of γ-rays and moderate neutrons, 5-cm of Pb and 7.5-cm high density polyethylene, HDPE, were placed between the scintillator and the source. Charge integration was used as a discrimination method where the difference in the amount of delayed light generated by proton and electron recoil is used to identify neutron and γ-ray events.

Experiments were conducted with scintillator samples of 2.5-cm diameter and 1-cm thickness. Scintillators were coupled to a Hamamatsu 2-inch R6231-100 photomultiplier with photocathode maximum sensitivity at 420nm. This PMT is well matched to the wavelength of maximum light emission for the developed scintillators. Signals from the E1198-27 photomultiplier base were transmitted to a 14-bit, 200 MHz 14200Gage Compuscope digitizer. Full waveforms were collected and analyzed offline. Energy calibration was performed using 662keV γ-rays from ^{137}Cs source assuming Compton edge energy of 478keV$_{ee}$ at 90% height of Compton edge distribution. PSD optimization was performed for events in the 50-100keV$_{ee}$, the energy range in which thermal neutron signature is presented with the highest intensity. The equation for the PSD is given by:

$$PSD = \frac{\sum_{del_{start}}^{del_{end}} Qdt}{\sum_{tot_{start}}^{del_{end}} Qdt}, \tag{2}$$

where del_{start} and del_{end} are respectively the beginning and end of the gate used for integration of charge generated due to delayed light, while tot_{start} corresponds to the beginning of the gate used for integration of total (prompt and delayed) charge. The beginning of the gate used for total charge integration was fixed at fourteen samples (70 ns) before the maximum peak amplitude. Integration of the delayed component was started 9 samples (45 ns) from pulse maximum and proceeded for 250 samples (1250 ns) to achieve the highest separation of neutron and γ-ray events in the energy range characteristic to thermal neutron capture. The integrated charge was corrected for the baseline, averaged over eighty pre-trigger samples. To quantify PSD, 1-D PSD distributions in energy bin of 50-100keV$_{ee}$ were used to calculate standard PSD figure-of-merit, FoM, according to

$$FoM = \frac{\langle n \rangle - \langle \gamma \rangle}{\Gamma_{FWHMn} + \Gamma_{FWHM\gamma}}, \tag{3}$$

where $\langle n \rangle$, $\langle \gamma \rangle$, Γ_{FWHMn}=2.35σ_n and $\Gamma_{FWHM\gamma}$=2.35σ_γ represent centroids and full-widths-at-half-maximum of Gaussian fits to the PSD distributions. Errors were calculated from propagation of parameter errors returned by the fitter.

Theoretical estimates of the performance of various ^{10}B-loadings have been obtained by performing MCNPX simulations using Neutron Capture Ion Algorithm (NCIA). All simulations have been carried out for 10^5 events, exposing scintillators with various concentrations of ^{10}B and thicknesses to thermal neutron flux (25meV). Neutron source of the size of scintillator area was set up with neutron initial direction normal to the detector face. Parameters effecting detector size, efficiency and resolving power, such as capture efficiency and average capture time, have been investigated across a range of ^{10}Boron concentrations. Histories were printed out on an event-by-event basis using ptrac card, and an algorithm was developed to post-process the ptrac file.

In order to calculate capture time, the time difference between thermal neutron injection into scintillator and alpha particle emission upon neutron capture were used to generate capture time distribution. The average capture time was calculated by performing an exponential fit to the distribution.

Thermal neutron capture efficiency was calculated using pulse height tally (f8) to group events in energy bins for alpha particles produced in the capture reaction, ensuring that the neutron is captured and alpha particle deposits all of its energy to the scintillator.

3. Results and Discussion

3.1. Pulse Shape Discrimination

Transparent, colorless samples (see Fig. 1) of PSD plastic scintillators containing from 0.4 to 5 wt.% of m-carborane with natural boron abundance were produced. The concentrations used (0.4; 0.75; 2.0; and 5.0 wt.%) correspond to ^{10}B content of (0.06; 0.11; 0.30; and 0.74 wt.%). Their performance in terms of light collecion efficiency and pulse shape discrinimation was studied in comparison to a control sample, a PSD plastic prepared under the same conditions without boron.

In order to identify scintillator signatures specific to the type of radiation, energy calibrated pulse shape discrimination (PSD) is illustrated in Fig. 2 a) and b) for a PSD plastic scintillator and its loaded analogue containing 5wt.% of m-carborane, respectively. The PSD plastic exhibits

Figure 1: PSD plastic scintillator samples containing 5wt.% of m-carborane with natural boron abundance.

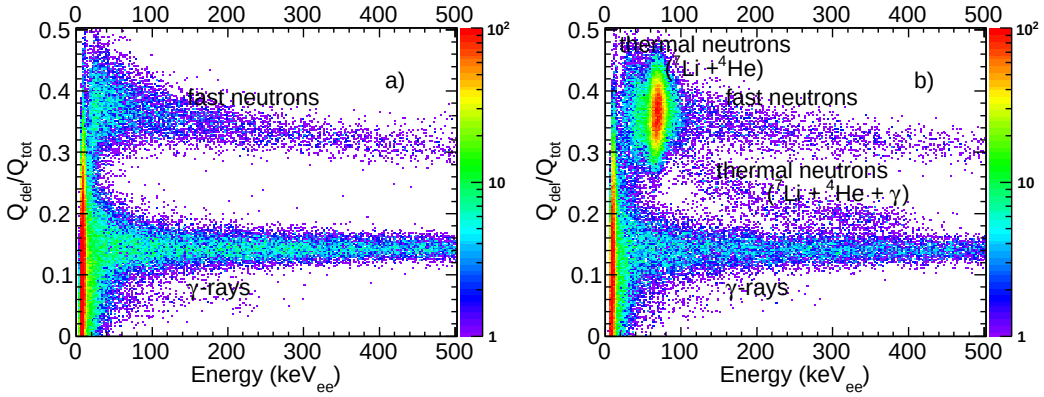

Figure 2: Pulse shape discrimination vs energy in electron equivalent units for a) PSD plastic exposed to neutron flux from 15-μCi ^{252}Cf source shielded with 7.5-cm of high density polyethylene (HDPE) and 5-cm of lead, b) plastic containing 5wt.% of m-carborane with natural abundance of boron under the same experimental conditions. Intensities, normalized with respect to time and solid angle coverage, can be used for efficiency comparison. Color scale represents counts.

typical response to γ-rays and fast neutrons, illustrated by two bands. The lower band, characteristic of smaller amount of delayed light, represents γ-ray events (scattered electrons). The upper band, with about 30-40% higher amount of the delayed light, exhibits a pattern characteristic to fast neutrons (recoiled protons). PSD plastic containing boron provides a response characteristic to thermal neutrons in addition to the typical signatures of γ-rays and fast neutrons. It should be noted that in thermal neutron capture reaction on ^{10}B, two branches are expected according to Eq. 1 giving rise to two different signatures. The first type corresponds to energy deposition by ^{7}Li+^{4}He. Because of constant energy of the charged reaction products defined by reaction kinematics and their short range of interaction, light output and its delayed fraction is well reproducible as illustrated by a signature with a mean of 72.6$\pm$0.01keV$_{ee}$ and 0.387$\pm$0.0003 in energy and PSD in Fig. 2 b), respectively. The second type of thermal neutron signature represents events characteristic to energy deposition of ^{7}Li+^{4}He and a capture γ-ray. Incident γ-rays on organic scintillator interact mainly by Compton scattering, and their energy deposition depends on scattering angle with maximum characteristic to Compton edge (313keV for 480keV capture γ-ray). Since scintillator response time is slower than γ-ray transit time, light output is a convolution due to excitation by charged reaction products and the capture γ-ray. Both, total light output and its delayed fraction varies depending on the capture γ-ray energy deposition. The ratio of delayed light is decreasing as the energy deposition is dominated by the capture γ-ray. Therefore, the second signature, characteristic to thermal neutrons, is shown as a band extending towards typical γ-ray signature. Its maximum energy corresponds to the sum of capture γ-ray Compton Edge energy and total energy deposition by charged reaction products (see Fig. 2 b)). Although 480keV γ-ray is emitted with 94% probability, the vast majority of the capture γ-rays escapes without depositing any energy to the scintillator due to the small sample size (2.5-cm diameter and 1-cm thickness), which is consistent with the two orders of magnitude higher intensity observed in the thermal neutron spot than in the band.

PSD distributions in the energy range 50-100keV$_{ee}$ are illustrated in Fig. 3 a) and b) for a PSD plastic and a B-loaded PSD plastic, respectively, to show the degree of neutron-γ separation and effect of boron loading on neutron detection efficiency. For each sample in Fig. 3 distributions are shown with and without external moderator (Pb+HDPE, and only Pb, respectively). These results indicate comparable scintillator performance in

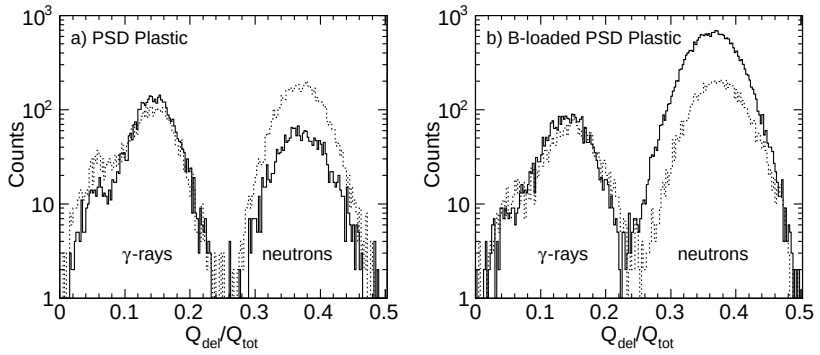

Figure 3: PSD distributions in energy range 50-100keV$_{ee}$ corresponding to data illustrated in Fig. 2 for a) unloaded PSD plastic, and b) PSD plastic containing 5wt.% of m-carborane with natural boron abundance. Dotted line distributions, obtained for samples exposed to 15-μCi ^{252}Cf source without additional moderator, show comparable intensity for both samples. Distributions represented by full lines, obtained with 7.5-cm of moderator (HDPE), illustrate significant increase in neutron counts for boron-loaded plastic compared to PSD plastic sensitive only to fast neutrons. Integrals, normalized with respect to time and solid angle coverage, can be used for efficiency comparison.

the absence of thermal neutrons, and significant gain in neutron detection capability in the case of boron-loaded PSD plastic as compared to unloaded PSD plastic exposed to moderated neutron flux. Figure 4 illustrates neutron-γ discrimination performance of boron-loaded plastic scintillator in 100keV$_{ee}$ energy bins for a range of energies from 100 to 500keV$_{ee}$. The distributions show clear separation between fast neutrons and γ-rays but partial overlap between thermal neutrons and γ-rays for events where the capture γ-ray undergoes scattering in the scintillator.

Additional studies were conducted on boron-loaded liquid scintillators to investigate PSD limits. The liquid scintillators were used for research purposes because of lower cost, easiness and short lead time for preparation of various compositions. Results are shown in Figs. 5-6 for xylene-based liquid scintillator containing 1wt.% of DPA (9,10-diphenylanthracene) and 1wt.% of boron oxide (III), enriched in ^{10}B, dissolved in 20wt.% of methanol). PSD figure-of-merit in energy range characteristic to thermal neutrons (see Fig. 6 a)), 50-100keV$_{ee}$, is 1.67$\pm$0.01 which is 20% higher than for typical plastics in the same energy range (1.4$\pm$0.03). The results also indicate that the clear signal due to ^{7}Li+^{4}He and a capture γ-ray could help better estimate the total number of neutron capture events statistically. It also should be noted

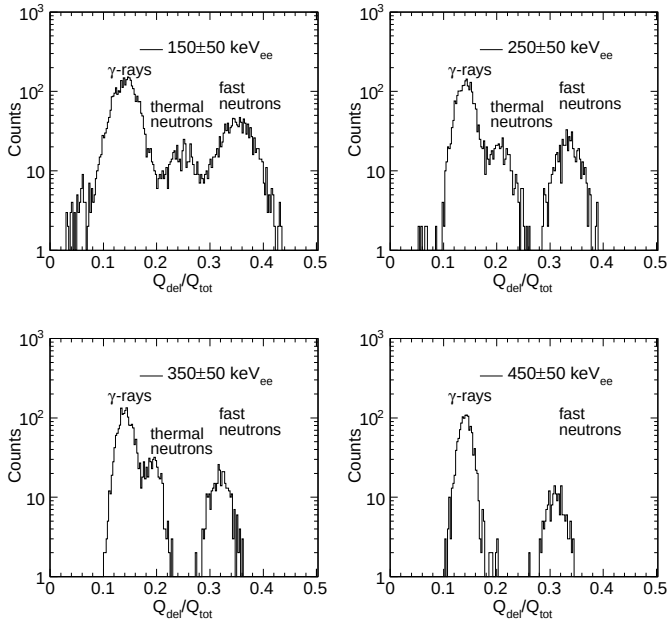

Figure 4: PSD distributions in several energy bins for PSD plastic containing 5wt.% of m-carborane. A sample of 2.5-cm diameter and 1-cm thickness was exposed to neutron flux from 15-μCi ^{252}Cf source shielded with 7.5-cm of high density polyethylene (HDPE) and 5-cm of lead.

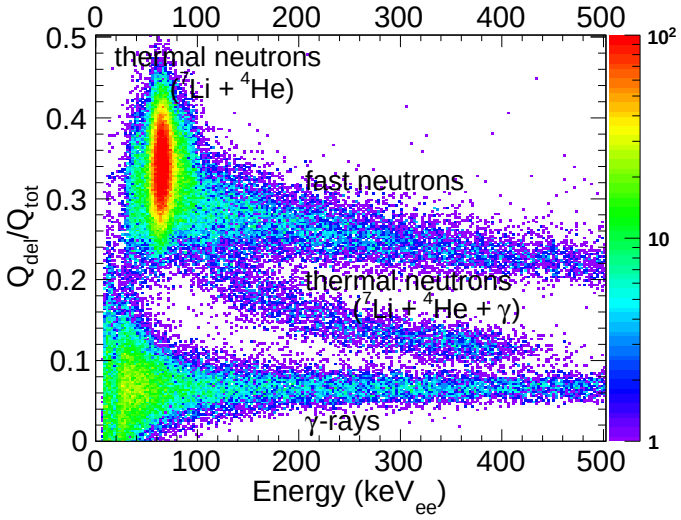

Figure 5: Pulse shape discrimination vs energy in electron equivalent units for a xylene-based liquid scintillator containing 1wt.% of DPA (9,10-diphenylanthracene) and 1wt.% of boron oxide (III) dissolved in 20wt.% of methanol. A sample of 5-cm diameter and 2.5-cm thickness was exposed to neutron flux from 15-μCi ^{252}Cf source shielded with 7.5-cm of high density polyethylene (HDPE) and 5-cm of lead. Color scale represents counts.

that the liquid scintillator provides a significantly better discrimination level than the currently available commercial scintillators [12, 13, 14, 15].

3.2. Effects of boron concentration

Incorporation of m-carborane into the scintillator requires careful understanding of effects of a boron-containing compound on the scintillator light collection and pulse shape discrimination properties. Therefore, plastic scintillator development was performed by balancing neutron detection efficiency, time properties and light yield in connection with ^{10}B concentration.

Light yield dependence measured in response to ^{137}Cs source on m-carborane concentration relative to a control sample shows a moderate decrease as illustrated in Fig. 7 a). A decrease of 20% in the light yield for a PSD plastic loaded with 5wt.% of m-carborane was found. However, it is the light yield generated by capture reaction products that is of particular interest for the scintillator under development. It is needed to estimate if there are additional light losses due to quenching in presence of reaction products. Therefore, the capture reaction products light yield was obtained by performing Gaussian

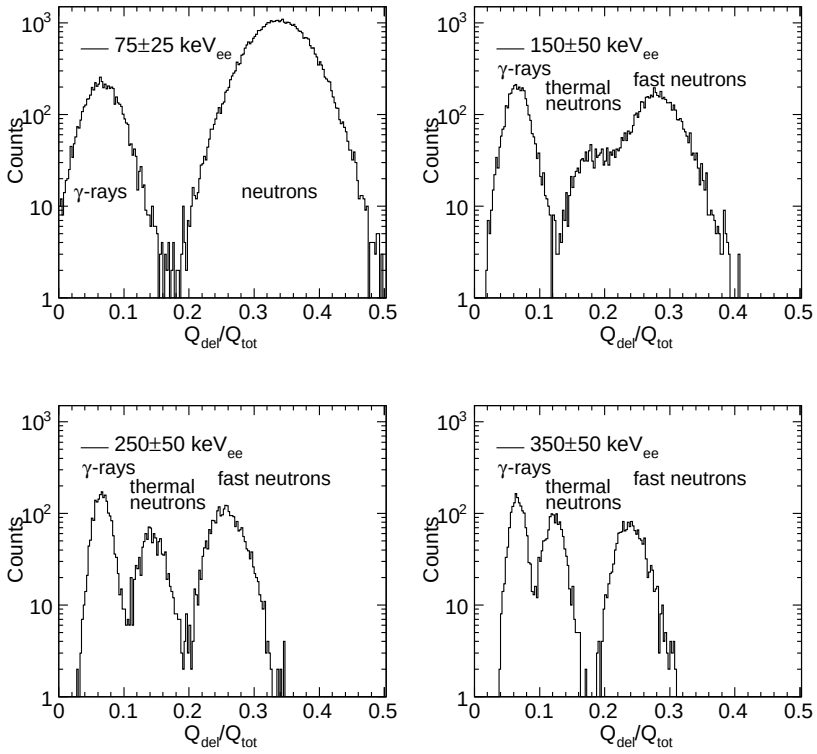

Figure 6: PSD distributions in several energy bins obtained with xylene-based liquid scintillator containing 1wt.% of DPA (9,10-diphenylanthracene) and 1wt.% of boron oxide (III), enriched in ^{10}B, dissolved in 20wt.% of methanol. A sample of 5-cm diameter and 2.5-cm thickness was exposed to neutron flux from 15-μCi ^{252}Cf source shielded with 7.5-cm of high density polyethylene (HDPE) and 5-cm of lead.

fits to the charge deposition characteristic to thermal neutron capture signature in pulse integral spectra. As a reference PSD plastic with 0.75wt.% of m-carborane loading was used. The results were compared to data obtained with ^{137}Cs source in Fig. 7 b). No additional losses were found for the capture reaction products, which is consistent with reduced light transmission due to attenuation rather than quenching.

Effects of m-carborane loading on neutron-γ discrimination properties, separation and figure-of-merit (FoM) values have been studied in energy domain characteristic to thermal neutrons 50-100keV$_{ee}$. Results illustrated in Fig. 7 c) show that separation remains constant across the range of m-carborane concentrations, which indicate that m-carborane does not affect the PSD process. Figure-of-merit values, on the other hand, slightly decrease with increasing m-carborane concentration, from 1.6 without boron loading to 1.4 with 5wt.% of m-carborane, respectively. The reason behind the decrease in the FoM is widening of neutron and γ PSD distributions due to light losses. For that purpose, the trend for full widths at half maximum, Γ_{FWHM}, is plotted in Fig. 7 d). This result is consistent with previous finding of moderately increasing light loss with increasing m-carborane concentration.

3.3. Simulation Predictions

Scintillator experimental development was combined with Monte Carlo calculations to estimate target ^{10}B concentration based on capture time and thermal neutron capture efficiency. Results of these calculations are presented in Figs. 8-10. It should be noted that the results of theoretical predictions obtained with MCNPX will be affected by scintillator neutron-γ discrimination levels which depend on many factors, including but not limited to count rate, scintillator size, setup components and their operation conditions; pmt, base, digitizer, sample rate, cable length [19], and should be evaluated experimentally as a part of calibration.

Capture time has been calculated as the time difference between thermal neutron injection into scintillator and the neutron capture. Calculated average capture times, $\langle t_c \rangle$ indicate a decrease of $\langle t_c \rangle$ from 10.2$\pm$0.03 to 0.9$\pm$0.002μs with increasing ^{10}B concentration from 0.1 to 2.0 wt.%. A slow response can be desirable at high incident neutron count rates, however; the detector will be more susceptible to accidental background. On the other hand, a faster detector response implies a shorter diffusion delay of neutron capture and is more desirable for applications with low neutron count rates such as the search for illicit trafficking of SNM. In addition, scintillator decay

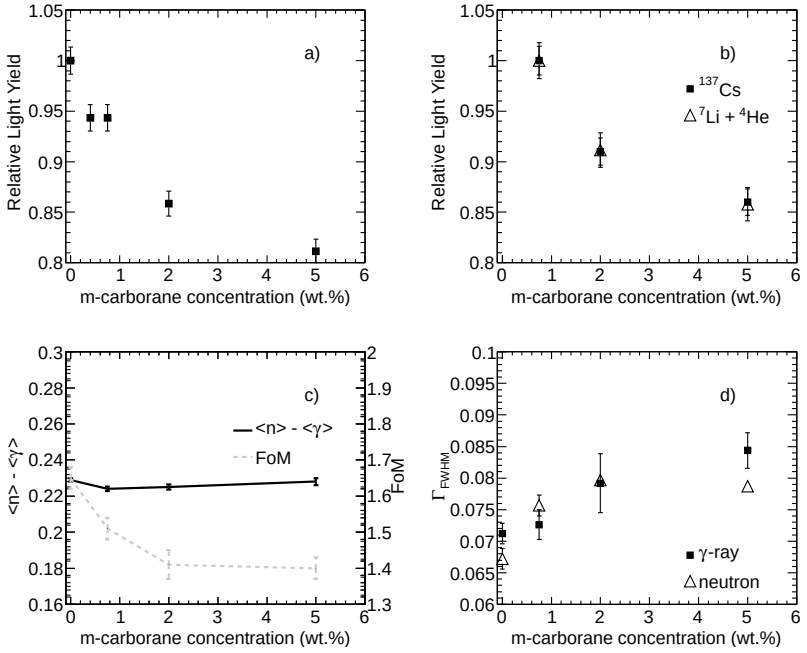

Figure 7: a) Light yield of PSD plastic samples containing various concentrations of m-carborane with natural boron abundance relative to a blank sample (PSD plastic), measured for ^{137}Cs. b) Light yield of PSD plastic samples loaded with various concentrations of natural m-carborane relative to a PSD plastic loaded with 0.75wt.% determined for thermal neutron capture reaction products. Comparison to the results obtained for ^{137}Cs source shows no additional light loss for capture reaction products. c) Neutron-γ separation and PSD figure-of-merit (FoM) vs m-carborane concentration. Separation is not influanced by m-carborane concentration while FoM shows slight decrease with increasing concentration due to moderate light loss. Lines are included to guide the eye. d) Full Width at Half Maximum (Γ_{FWHM}) of neutron and γ PSD distributions in energy range 50-100keV$_{ee}$ vs m-carborane concentration.

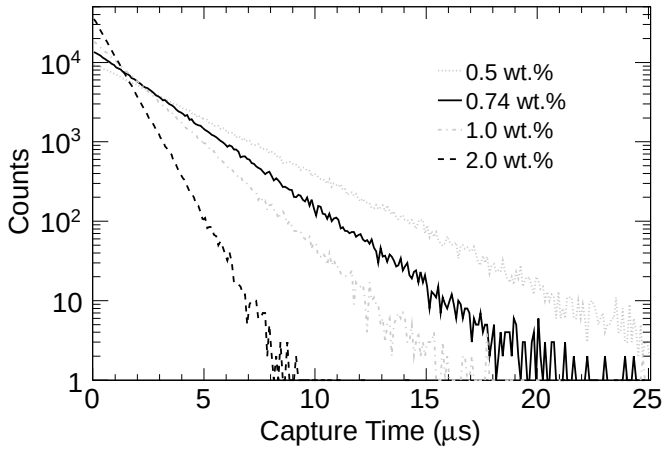

Figure 8: Simulated capture time distributions for PSD plastic containing concentrations of 0.5, 0.74, 1.0, and 2.0 of ^{10}Boron by weight.

characteristics should also be taken into consideration, particularly because in response to neutrons (thermal and fast) the PSD plastic scintillator emits a significant amount of delayed light required for effective PSD for approximately 1.3μs.

Simulated thermal neutron capture efficiency on ^{10}B, presented in Fig. 10, increases with scintillator thickness to reach saturation. Both, the slope and the efficiency at saturation depend on ^{10}B concentration. With increasing ^{10}B concentration, capture efficiency approaches, but does not reach, unity mainly due to thermal neutron escape at detector boundaries. For the considered scintillator sizes, only marginal losses were found due to competing capture reaction on ^{1}H nucleus. B-loaded PSD plastic scintillator response to the 2.2 MeV γ-rays, emitted upon thermal neutron capture on ^{1}H nucleus, will essentially result in a pulse with decay characteristic to γ-rays (recoiled electrons). Therefore, these thermal neutron capture events cannot be discriminated directly against background γ-rays. Generally, larger ^{10}B concentrations will provide smaller size, more efficient detectors with faster response to thermal neutrons. However, all the parameters depending on ^{10}B mentioned above need to be optimized for specific conditions and applications.

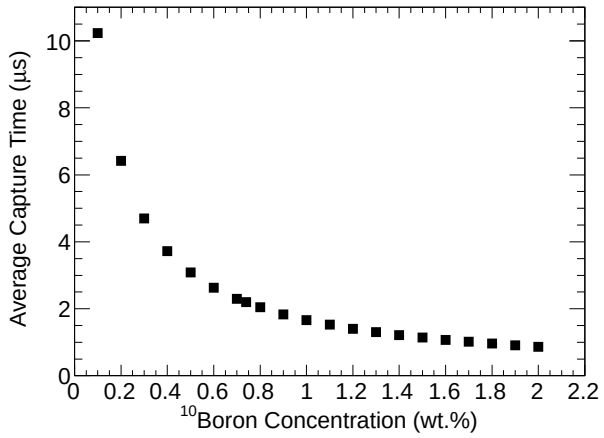

Figure 9: Simulated average neutron capture time vs ^{10}Boron concentration by weight. Error bars are within the points.

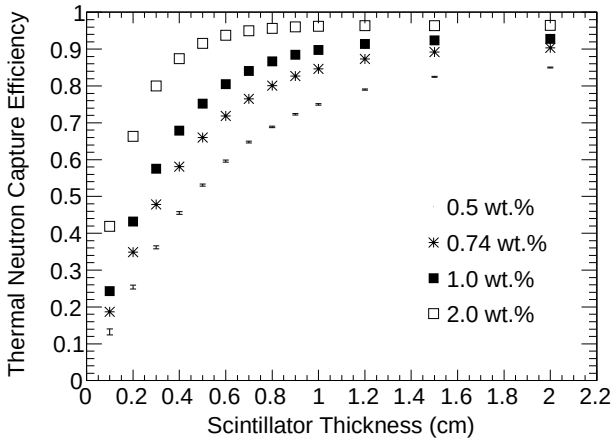

Figure 10: Simulated thermal neutron capture efficiency of ^{10}B vs scintillator thickness for ^{10}Boron loading of 0.5, 0.74, 1.0, and 2.0 % by weight. Error bars are within the points.

4. Conclusions

Development of pulse shape discriminating plastic scintillator for efficient neutron detection has been demonstrated by incorporation of m-carborane. The material introduces detector sensitivity to neutrons which are below the threshold for detection by proton recoil maintaining sensitivity to fast neutrons, while discriminating against γ-rays. This may be particularly important for passive detection of low flux neutron sources such as illicit nuclear material, where fission neutrons lose energy by scattering in shielding and the environment before entering the detector. Simulation results suggest that at 0.74% of ^{10}B loading thermal neutrons can be captured, on average, within 2.2μs with detection efficiency of 84% in 1-cm thick scintillator. Incorporation of 0.74wt.% of ^{10}B in the form of carborane with natural boron abundance requires 5% of carborane by weight, and does not influence the scintillator pulse shape discrimination properties beyond a moderate decrease of light yield. A PSD figure-of-merit value of 1.4±0.03 in the energy range of 50-100keV$_{ee}$ was obtained for PSD plastic loaded with 5wt.% of m-carborane by integration of the delayed light from 45ns to 1.25μs from maximum. A combination of experimental and simulation results suggest that boron-laoded PSD plastic is a good candidate for an efficient compact neutron detection system.

5. Acknowledgements

This work was performed under the auspices of the U.S. Department of Energy by Lawrence Livermore National Laboratory under Contract DE-AC52-07NA27344. Financial support provided by the U.S. Department of Energy Office of Nonproliferation Research and Development (NA-22) and Defense and Thread Reduction Agency. The authors wish to thank Dr. Benjamin Rupert for preparation of liquid scintillator and Dr. Ronald Wurtz for valuable discussions.

References

[1] N. Zaitseva, B.L. Rupert, I. Pawełczak, A. Glenn, H.P. Martinez, L. Carman, M. Faust, N. Cherepy, S. Payne, Nucl. Istr. Meth. A 668 (2012) 88.

[2] N. Zaitseva, A. Glenn, H.P. Martinez, L. Carman, I. Pawełczak, M. Faust, and S. Payne, Nucl. Istr. Meth. A 729 (2013) 747.

[3] G. Knoll, Radiation Detection and Measurements, third ed., Wiley, New York, (1999).

[4] D.M. Drake, W.C. Feldman, C. Hurlbut, Nucl. Istr. Meth. A 247 (1986) 576.

[5] J.B. Czirr, G.L. Jensen, Nucl. Istr. Meth. A 349 (1994) 532.

[6] J.B. Czirr, D.B. Merrill, D. Buehler, T.K. McKnight, J.L. Carroll, T. Abbott, E. Wilcox, Nucl. Istr. Meth. A 476 (1994) 309.

[7] S.D. Jastaniah, P.J. Sellin, Nucl. Istr. Meth. A 517 (2004) 202.

[8] I.A. Pawełczak, J. Toke, E. Henry, M. Quinlan, H. Singh, W.U. Schroeder, Nucl. Instr. Meth. A 629, (2011) 230.

[9] L.M. Bollinger, G.E. Thomas, Rev. Sci. Instr. 28, (1957) 489.

[10] H.E. Jackson, G.E. Thomas, Rev. Sci. Instr. 36, (1965) 419.

[11] L. Swiderski, M. Moszynski, D. Wolski, T. Batsch, A. Nassalski, A. Syntfeld- Kazuch, T. Szczesniak, F. Kniest, M.R. Kusner, G. Pausch, J. Stein, W. Klamra, IEEE Trans. Nucl. Sci. 55 (2008) 3710.

[12] M.Flaska, S.A. Pozzi, Nucl. Instr. Meth. A 599 (2009) 221.

[13] L. Swiderski, M. Moszynski, D. Wolski, T. Batsch, J. Iwanowska, A. Nassalski, A. Syntfeld-Kazuch, T. Szczesniak, F. Kniest, M.R. Kusner, G. Pausch, J. Stein, W. Klamra, P. Schotanus, C. Hurlbut, IEEE Trans. Nucl. Sci. 57 (2010) 375.

[14] L. Swiderski, M. Moszynski, D. Wolski, J. Iwanowska, T. Szczesniak, G. Pausch, C. Plettner, J. Stein, P. Schotanus, C. Hurlbut, J. Szabelski, IEEE Trans. Nucl. Sci. 57,(2010) 2857.

[15] T. Szczesniak, M. Moszynski, A. Syntfeld-Kazuch, L. Swiderski, D. Wolski, M. Grodzicka, G. Pausch, J. Stein, F. Kniest, M.R. Kusner, P. Schotanus, C. Hurlbut, IEEE Trans. Nucl. Sci. 57 (2010) 3846.

[16] L.M. Bollinger, G.E. Thomas, R.J. Ginther, Nucl. Instr. Meth. 17, (1962) 97.

[17] S. Normand, B. Mouanda, S. Haan, M. Louvel, IEEE Trans. Nucl. Sci. 49, (2002) 577.

[18] Z.W. Bell, M.A. Miller, L. Maya, G.M. Brown, F.V. Sloop, Jr., IEEE Trans. Nucl. Sci. 51,(2004) 1773.

[19] I.A. Pawełczak, S.A. Ouedraogo, A.M. Glenn, R.E. Wurtz, L.F. Nakae, Nucl. Instr. Meth. 711, (2013) 21.